Front. Phys. 10(5), 104207 (2015)
DOI 10.1007/s11467-015-0500-2

RESEARCH ARTICLE

Effect of parameters on Si plasma emission in collinear double-pulse laser-induced breakdown spectroscopy

Fang-Fang Chen, Xue-Jiao Su, Wei-Dong Zhou†

Key Laboratory of Optical Information Detection and Display Technology of Zhejiang, Zhejiang Normal University, Jinhua 321004, China

Corresponding author. E-mail: †*wdzhou@zjnu.cn*

Received March 29, 2015; accepted June 24, 2015

Collinear dual-pulse laser-induced breakdown spectroscopy was carried out on Si crystal by using a pair of nanosecond Nd:YAG laser sources emitting at 1064 nm. The spectral intensities and signal-to-noise ratios of selected Si atomic and ionic lines were used to evaluate the optical emission. The optical emission intensity was recorded while varying the interpulse delay time and energy ratio of the two pulsed lasers. The effects of the data acquisition delay time on the line intensity and signal-to-noise ratio have been investigated as well. Based on the results, the optimal interpulse delay time, energy ratio of the two pulsed lasers, and data acquisition delay time for achieving the maximum atomic and ionic line intensities were found for generation of Si plasma with the collinear dual-pulse laser approach. The dominant mechanism for the observed line intensity variation was also discussed. In addition, the plasma temperature and electron number density at different gate delay times and different interpulse delay times were derived. A significant influence of plasma shielding on the electron temperature and electron number density at shorter interpulse delay times was observed.

Keywords laser-induced breakdown spectroscopy, collinear dual-pulse, plasma emission intensity

PACS numbers 42.62.Fi, 52.25.Os, 52.50.Jm

1 Introduction

Laser-induced breakdown spectroscopy (LIBS) is well known as a valuable analytical technique for qualitative and quantitative determination of the elemental compositions of different types of materials, either in gaseous, liquid, or solid phase, with the advantage of performing non-contact measurements without significant requirements for sample preparation [1–3]. However, compared with other spectroscopy methods, LIBS always suffers from a relatively poor sensitivity and measurement uncertainty, which in turn restricts its further analytical application. In order to improve the detection capability and increase the sensitivity of LIBS, a number of methods, including discharge enhancement [4–6], plasma confinement [7–9], and the use of dual-pulse (DP) laser excitation [10–12], have been proposed. Among these methods, the most common approach is probably the DP-LIBS in which the second laser pulse is focused onto the plasma produced by the first pulse to enhance the plasma emission. Basically, two experimental configurations have been adopted in the DP-LIBS technique, a collinear dual-pulse configuration and an orthogonal dual-pulse configuration. Both have been used to successfully enhance the plasma emission intensity and signal-to-noise ratio. To date, much research has addressed the enhancement mechanism. For DP-LIBS in the collinear geometry, as suggested by Sattmann *et al.* [13], the atomic emission enhancements resulted from a combination of improved ablation, increased electron densities, and higher plasma temperature. However, in fact, the signal enhancement in DP-LIBS was strongly dependent on the specific experimental conditions and parameters they adopted in their studies [10, 13]. For each experiment and specific application of DP-LIBS, a parameter optimization is then necessary to get the best performance. On the other hand, to date, most of the DP-LIBS research has focused on the enhancement of dual-pulse laser ablation of metal samples, and only rarely has the focus been the plasma enhancement of dual-pulse laser ablation of dielectric material; it would therefore be interesting to know how the dual-pulse laser ablation affects the laser plasma character of a dielectric material.

In this article, a dielectric sample (Si crystal) is used to investigate the plasma emission character of collinear dual-pulse laser-induced plasma. The optical emission intensity and stability of the plasma are investigated under different interpulse delay times and energy ratios of the two pulse lasers. The optimum gate delay time and interpulse delay time corresponding to the maximum value of the emission signal are observed. Based on these results, the signal enhancement mechanisms are discussed.

2 Experiment

A schematic diagram of the experimental setup of DP-LIBS is shown in Fig. 1. Two identical Q-switched Nd:YAG lasers, both operated at a wavelength of 1064 nm with a pulse width of 10 ns and a repetition rate of 1 Hz, are combined in a collinear beam geometry, similar to that reported previously [14]. The laser energy can be adjusted continuously from 0 to 180 mJ, depending on the experimental requirements. During the experiments, the lasers were focused on the surface of a silicon crystal (with beams normal to the crystal surface) by a convex lens of focal length 50 mm, and the lens-to-sample distance was set to be 1 mm less than the focal length, in order to avoid the breakdown of air in front of the target and to improve the stability of the plasma. All the experiments were carried out under normal atmospheric conditions, and the total energy of the two laser pulses was set to be 40 mJ. The surface of the Si crystal was polished and cleaned prior to ablation. The interpulse delay time Δt between the two laser pulses and the data acquisition delay time (gate delay) t_d of the spectrometer, which was the time delay between the first laser pulse and the start of the recording of the spectrum, were controlled by a digital pulse delay generator (Model DG535, Stanford Instruments), which has a time resolution of 1 ns. So the time delay between the two lasers and the collection of the light can be controlled precisely.

The optical emission from the plasma was collected by using a collimating lens at an angle of 45° to the laser beam. A bundle of 200-μm-diameter, multimode optical fibers was used to deliver the collected light to an Avaspec-2048 fiber optic spectrometer. The spectrometer provided an average spectral resolution of ~0.1 nm (full width at half maximum, FWHM) in a broad continuous spectral range between 196 and 500 nm. The detector was a CCD linear array consisting of 2048 pixels; the detector can be externally triggered to initiate spectroscopy recording with an integrating time of 2 ms. In order to increase the signal-to-noise ratio (S/N) and improve the precision of the measurements, for each experiment, 100 spectra were collected, and all the spectra presented here represent averages over 20 spectra. Such an averaged spectrum then served as a single measurement, and so 5 such independent repeated measurements were carried out for each experiment and were used for deriving the relative standard deviation (RSD) of the measured line peak intensity. In the experiment, the Si-crystal sample was mounted on a motorized X-Y translation stage in order to ablate a fresh spot for each dual-pulse-laser excitation.

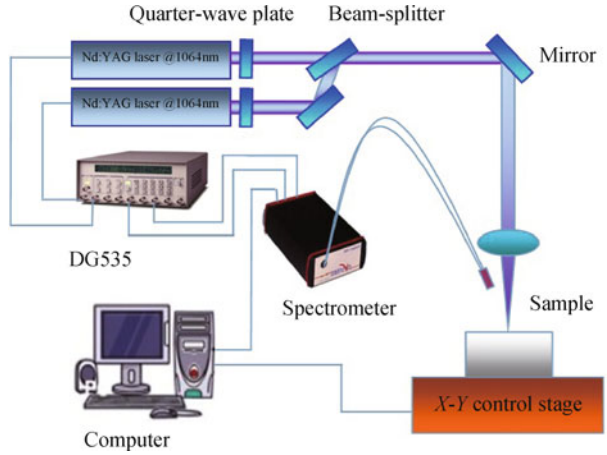

Fig. 1 Schematic diagram of the experimental setup for double-pulse experiment in the collinear geometry.

3 Results and discussion

3.1 Influence of the interpulse delay time

As pointed out by other researchers, the interpulse delay time is actually a dominant parameter in determining the plasma emission intensity. Figure 2 shows the typical spectra of the Si plasma emission measured at interpulse delay times of 0 μs and 1 μs, respectively, with the same gate delay time 1 μs. The spectrum in the inside panel (C) was produced by dual-pulse excitation with an interpulse delay time of 1 μs. In contrast, the spectrum in the outside panel (D) was obtained under similar experimental conditions except that the interpulse delay time was 0 μs. The laser energy is 20 mJ per pulse for both laser beams. From Fig. 2, it is clear that the spectral intensity with the 1-μs interpulse delay time was significantly higher than that of the 0-μs interpulse delay time. This may be attributed to the difference in plasma evolution under different interpulse delay times. Dual-pulse laser-induced plasma with a 0-μs interpulse delay time is actually equivalent to single-pulse laser-induced plasma with equal total laser energy. In this case, the laser-induced plasma evolution has only gone through two

steps: the laser induces a plasma and generates a shock wave, and then the plasma plume expands and decays. In contrast, for the dual-pulse laser-induced plasma with longer interpulse delay time, the laser-produced plasma will undergo a more complicated process. Initially, the first laser beam induces a plasma, and then the produced plasma decays. Next, the second laser beam reheats the first laser plasma and increases both the plasma temperature and the electron number density, leading to enhancement of the signal intensity. In addition, the second laser beam will ablate the sample again and generate a second plasma plume as well. Generally, there are two processes that may be plausibly occurring in the plasma plume of collinear DP-LIBS: (i) absorption of the second laser pulse in the plume of the plasma initiated by the first laser pulse (reheating mechanisms) [10, 15], and (ii) new plasma formation by the remaining second laser pulse [16, 17]. In fact, the plasma absorption is actually lower than that of SP-LIBS with the same total laser energy in collinear DP-LIBS; thus, more laser energy can reach the target, increase the laser ablation, and enhance the line intensity [15]. It is hard to separate the effects of these two enhancement mechanisms, as the combination of these effects will have a significant impact on the signal enhancement as well. For example, the differences in the gas environments in SP-LIBS (air gas) and in DP-LIBS for the second laser pulse (i.e., the expanded plasma of the first laser ablation) will play an important role and will affect the energy flow and energy transfer to the environmental gas. In our experiment, the ablation efficiency of DP-LIBS is approximately 2 times higher than that of SP-LIBS. On the other hand, the contribution of reheating to the emission enhancement will depend on the interpulse delay time. At longer interpulse delay times, only the atoms and electrons in the waist volume of the second laser beam can absorb a portion of the laser energy. In contrast, at shorter interpulse delay times, the two pulses can couple to each other, allowing multi-photon effects, and the reheating effect will be higher.

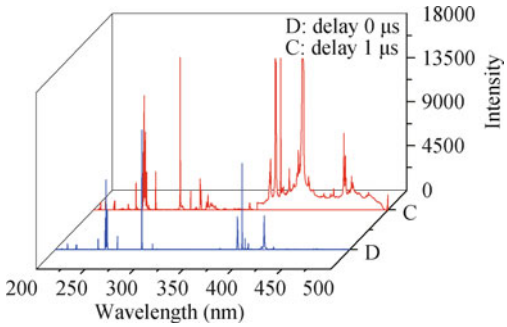

Fig. 2 Typical DP-LIBS spectra of Si plasma emission obtained at interpulse delay time 0 μs and 1 μs, both spectra were recorded at total laser energy 40mJ and gate delay 1 μs and an integration time 2 ms.

First, we optimized the interpulse delay time between the two laser pulses. Figure 3 shows the time-integrated line intensity versus the interpulse delay time between the two laser pulses for selected Si atomic and ionic transitions at different data acquisition delay (i.e., gate delay) times. When the two laser pulses have identical energies and for a given gate delay time, the emission intensities of all selected Si atomic and ionic lines increase rapidly during the initial phase of the time delay between the two pulses, reach a maximum value, and then gradually decrease at longer delay times.

It has previously been reported that the plasma reheating by the second laser significantly contributes to the plasma emission enhancement in collinear DP-LIBS [10, 11, 15]. Therefore the morphology of the plasma plume and the particle density in the region of interaction between the first laser plasma and the second laser beam will greatly affect the number of overall particles reheated by the second laser. Thus, an interpulse-delay-time–dependent line intensity enhancement was observed. At short interpulse delay times, similar to those in SP-LIBS, because of the plasma shielding and plasma absorption, the ablation efficiency and ablated mass will be lower than those of longer interpulse delay times; that is why a relatively lower line intensity was observed at short interpulse delay times. On the other hand, if the interpulse delay time is long enough, along with the outward expansion of the first laser plasma plume, the electron and ion number densities of the first laser plasma will become steadily lower in the path of the second laser beam. Therefore, the effect of plasma shielding and plasma absorption of the first laser plasma on the second laser beam will decrease compared with that for shorter interpulse delay times. In this case, the laser plasma is likely to be more similar to two independent laser plasmas. The advantages of the dual-pulse laser excitation effect then become steadily less, and so the line intensity decreases again. It is interesting to note that, for shorter gate delay times (0 μs, 0.5 μs, and 1.5 μs), the maximum signal intensity occurred at an interpulse delay time of ∼1.0gμs. In contrast, for longer gate delay times (3.5 μs, 5.5 μs, and 7.5 μs), the interpulse delay time to obtain the maximum line intensity is dependent on the gate delay time and actually is roughly around the gate delay time. This is because with a longer gate delay time, if the second laser pulse arrives before the gate of the spectrometer opens, because of plasma evolution, the most intense plasma emission cannot be recorded. Therefore, in this case, the best interpulse delay time for recording the intense signal is roughly equal to the gate

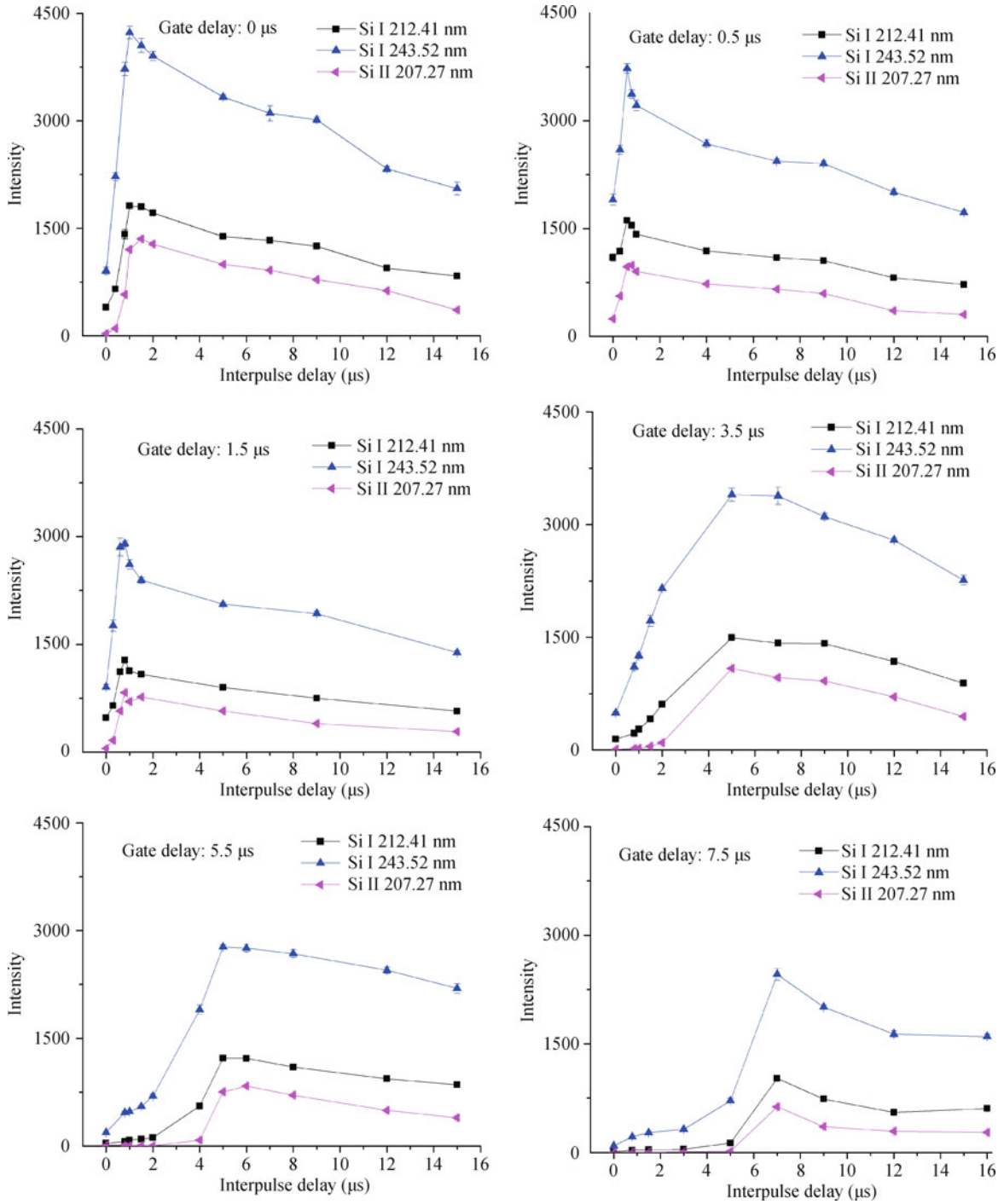

Fig. 3 Interpulse delay dependence of the emission intensities of selected Si lines at six different gate delay time t_d (E = 20 mJ + 20 mJ).

delay time.

3.2 Influence of the gate delay time

Figure 4 shows the spectral line intensity at a fixed interpulse delay time of 1.5 μs but with different gate delay times. By increasing the gate delay time, a monotonously decreasing signal intensity was observed. In contrast, the signal-to-noise ratio first increased at shorter gate delay times and then gradually decreased at longer gate delays, and it showed a maximum at a gate delay time of ~1 μs. As the CCD integration time (2 ms) is longer than the DP-laser plasma lifetime (~10 to 100 μs), the earlier the gate opens, the more signal will be integrated, and so a more intense signal will be observed at shorter gate delay times. In contrast, for the signal-to-noise ratio, as the

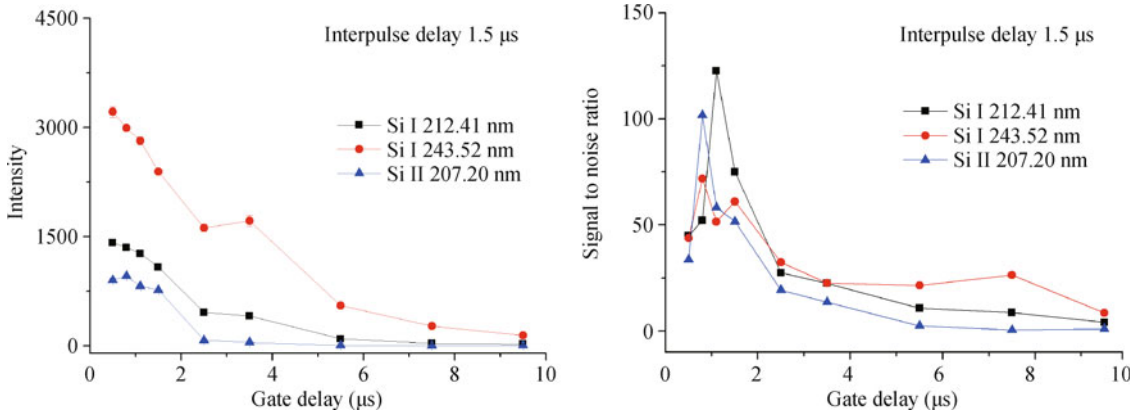

Fig. 4 Evolution of line intensity and signal-to-noise (S/N) ratio vs. different gate delay time.

intense background and noise appear during the early stage of the laser plasma, the optimized value was observed at later gate delay times.

3.3 Influence of the dual-pulse energy ratio

Here we describe our study on the effect of the ratio of the two different laser pulse energies in collinear DP-LIBS on the line intensity. Figure 5 shows the spectral intensity and the signal-to-noise ratio as a function of the ratio of the two laser pulse energies. The experiment was performed by continuously changing both the laser pulse energies in such a way that the total energy remains the same but with different energy ratios (1:3, 1:2, 1:1, 2:1, and 3:1), without changing the interpulse delay of 1.0 μs and the gate delay of 1 μs. It was interesting to note that the maximum signal intensity and signal-to-noise ratio were observed when the two laser pulse energies were equal.

The effect of the energy ratio on the line intensity in collinear DP-LIBS has been previously reported. Rai *et al.* [18] used the collinear DP configuration and found that the maximum signal intensity occurs when the energy of the first pulse is set to 100 mJ and that of the second pulse is set to 120 mJ. This result is close to that which we obtained here. Benedetti *et al.* [19] studied the effect of laser pulse energies in a DP-LIBS spectrum using an aluminum sample by fixing the second laser pulse energy at 78 mJ and changing the first pulse energy from 13 to 78 mJ. The results showed that maximum enhancement occurs when the energy of the first laser pulse is a third of that of the second laser pulse. Rashid *et al.* [20] used a collinear DP-induced silver plasma and remarked that the maximum intensity for the Ag I 546.55-nm line occurred when the energy of the delayed laser pulse was about 2.5 times the energy of the first laser pulse. It is likely that the different values for the correct energy ratio for obtaining the maximum signal intensity found through different research efforts result from differences in experimental parameters. For example, the different laser energies and focus conditions will change the electron and ion number densities in the first laser plasma, and therefore change the plasma shielding effect for the subsequent laser pulse. In addition, the surface roughness

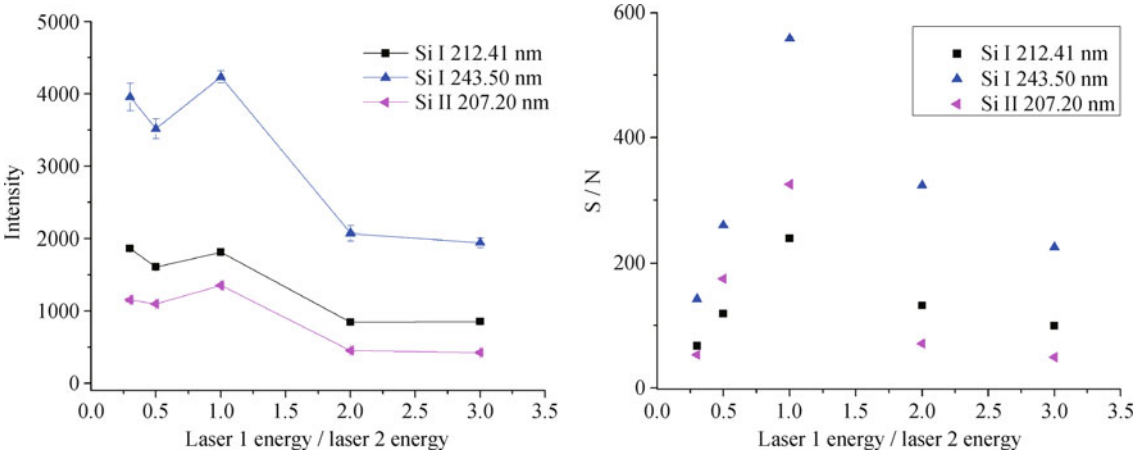

Fig. 5 The variation of signal intensity and S/N ratio as a function of laser pulse energies ratio.

and thermal characteristics of the used sample will contribute to the disagreement, as the sample characteristics in turn will significantly affect the laser energy being absorbed by the sample and therefore affect the ablation process. There exists an optimized energy ratio for collinear DP-LIBS, the value of this ratio depends on the specific experimental condition and the used sample. It is therefore inferred that by optimizing the ratio of the laser pulse energies as well as the interpulse delay time between the two laser pulses, one may achieve the maximum signal intensity and signal-to-noise ratio for the collinear DP-LIBS technique.

3.4 The temperature and electron number density

The plasma parameters such as electron temperature and electron number density provide important information regarding the characterization of laser-induced plasmas and their applications. Under thermodynamic equilibrium, temperature can be estimated based on the plasma emission line intensity. However, in practice, thermodynamic equilibrium is rare, so very often the useful approximation of local thermodynamic equilibrium (LTE) is adopted so that the plasma temperature and electron number densities can be calculated from the spectroscopy measurements. Under the LTE assumption, the plasma temperature T can be calculated from the intensity ratio of two Si I lines that have different upper energy levels [21, 22]. That is,

$$T = \frac{E_2 - E_1}{k}\left[\ln\left(\frac{I_1\lambda_1 g_2 A_2}{I_2\lambda_2 g_1 A_1}\right)\right]^{-1} \quad (1)$$

where E_1 and E_2 are the energies of the upper transition levels of two lines belonging to the same atomic species, and $k$is Boltzmann's constant. I_1 and I_2 are the line intensities of the two lines; A_1, g_1, and λ_1 are the transition probability, degeneracy, and wavelength, respectively, of one spectral line, whereas A_2, g_2, and λ_2 correspond to the same quantities for the other emission line of the same species. Table 1 includes the spectroscopic parameters for Si atomic emission lines, obtained from Ref. [23]. The excitation temperature is derived using the Si atomic line intensities for Si I 263.13 nm and Si I 243.52 nm at different gate delay times and at different interpulse delay times for collinear DP-LIBS. In order to minimize the effect of self-absorption on the temperature calculation, two non-resonant and relatively less intense lines are selected and used for the calculation. The results are shown in Table 2.

For the DP-laser plasma with the same interpulse delay time, although the gate delay times were different, no significant difference in plasma temperature evolution were found. Furthermore, an approximately equal value of the electron temperature (∼14 000 K) was observed for collinear DP-laser plasma with interpulse delay times of 0.5 μs, 1 μs, and 1.5 μs. However, for a 0-μs interpulse delay time, the electron temperature was much lower, and the value is approximately ∼7500 K. This is consistent with the observation that dual-pulse LIBS can significantly increase the plasma temperature [13, 16, 17, 24].

Table 1 Line parameters used for determining electron temperature.

λ_{ki} (nm)	E_K (cm^{-1})	E_K (eV)	g	$A_{ki}(10^8 s)$
Si I 243.52	47351.554	5.87	5	0.443
Si I 263.13	53387.334	6.62	3	1.060

Table 2 Plasma temperature (K) of collinear DP-LIBS at different gate delay time and interpulse delay time.

Interpulse delay \ Gate delay	0 μs	1 μs	2 μs	3 μs
0 μs	8534.56	8286.754	7998.573	7551.085
0.5 μs	13734.23	14029.56	15288.97	13703.47
1 μs	13725.23	13056.95	14554.61	15249.32
1.5 μs	13499.36	13521.99	14497.77	14220.06

The plasma electron number density can be approximately calculated by Stark broadening of a spectral line profile and using the expression [21, 25]

$$\Delta\lambda_s = 2\omega \times \frac{N_e}{10^{16}} \quad (2)$$

where ω is the Stark broadening parameter and $\Delta\lambda_s$ is the half-width half-maximum (HWHM) of the Stark profile of the considered transition line, which can be derived from the experimentally measured linewidth by taking into account the instrumental broadening and Doppler broadening. The experimentally obtained plasma electron number density values at different gate delay times after the first laser irradiation and at different interpulse delay times are shown in Table 3, where we have used the Stark-broadened line profiles of Si I 212.41-nm lines. As with the electron temperature, a significantly different value of the number density was observed for collinear DP-laser plasma with a 0-μs interpulse delay time, compared to the number densities for interpulse delay times of 0.5 μs, 1 μs, and 1.5 μs. However, for the same interpulse delay time, the number density decreases slightly along with the gate delay time, in contrast with the behavior of the of plasma temperature observed above. Because of the plasma shielding and absorption, the electron temperature and number density will be significant affected at shorter interpulse delay times. However, at longer interpulse delay times, the plasma shielding effects probably can be neglected.

Table 3 Electron number densities N_e (units, $10^{17}/cm^3$) of collinear DP-LIBS at different gate delay time and interpulse delay time.

Interpulse delay \ Gate delay	0 μs	1 μs	2 μs	3 μs
0 μs	5.975	5.517	4.836	4.803
0.5 μs	8.91	8.602	6.415	6.056
1 μs	8.78	8.817	6.307	6.162
1.5 μs	7.841	8.856	7.007	5.905

4 Conclusion

In this article, the optical emission of collinear dual-pulse laser-induced Si plasma was investigated and used to realize the advantage of and maximize the signal enhancement in DP-LIBS. Obvious enhancement of optical emission was observed. The effects of the interpulse delay time, the gate delay time, and the energy ratio of the energies of the two laser pulses on the signal intensity and signal-to-noise ratio were carefully investigated. Based on these results, the optimized parameters for achieving the maximum atomic and ionic line intensities were found for collinear DP-LIBS. These maximum values occur when both the interpulse delay time and gate delay time are about 1 μs, and when the energy of the delayed laser pulse is about equal to the energy of the first laser pulse. A few silicon atomic line intensities and the Stark broadening of the Si I 212.41-nm lines were measured and used to derive the electron temperature and electron number density under different interpulse delay times. A significant influence of plasma shielding on the electron temperature and the electron number density was observed.

Acknowledgements This study was supported by the National Natural Science Foundation of China (Grant No. 61178034), the Natural Science Foundation of Zhejiang Province (Grant No. LY14F050003), and was partially supported by the Program for Innovative Research Team, Zhejiang Normal University, China.

References

1. J. P. Singh and S. N. Thakkur, Laser-Induced Breakdown Spectroscopy, Elsevier Science, Oxford, 2007
2. Z. Wang, T. B. Yuan, Z. Y. Hou, W. D. Zhou, J. D. Lu, H. B. Ding, and X. Y. Zeng, Laser-induced breakdown spectroscopy in China, *Front. Phys.* 9(4), 419 (2014)
3. J. S. Xiu, X. S. Bai, V. Motto-Ros, and J. Yu, Characteristics of indirect laser-induced plasma from a thin film of oil on a metallic substrate, *Front. Phys.* 10(2), 104204 (2015)
4. X. Li, W. Zhou, K. Li, H. Qian, and Z. Ren, Laser ablation fast pulse discharge plasma spectroscopy analysis of Pb, Mg and Sn in soil, *Opt. Commun.* 285(1), 54 (2012)
5. W. Zhou, K. Li, H. Qian, Z. Ren, and Y. Yu, Effect of voltage and capacitance in nanosecond pulse discharge enhanced laser-induced breakdown spectroscopy, *Appl. Opt.* 51(7), B42 (2012)
6. Z. Hou, Z. Wang, J. Liu, W. Ni, and Z. Li, Combination of cylindrical confinement and spark discharge for signal improvement using laser induced breakdown spectroscopy, *Opt. Express* 22(11), 12909 (2014)
7. A. M. Popov, F. Colao, and R. Fantoni, Enhancement of LIBS signal by spatially confining the laser-induced plasma, *J. Anal. At. Spectrom.* 24(5), 602 (2009)
8. Z. Wang, Z. Hou, S. Lui, D. Jiang, J. Liu, and Z. Li, Utilization of moderate cylindrical confinement for precision improvement of laser-induced breakdown spectroscopy signal, *Opt. Express* 20(23), A1011 (2012)
9. X. Su, W. Zhou, and H. Qian, Optimization of cavity size for spatial confined laser-induced breakdown spectroscopy, *Opt. Express* 22(23), 28437 (2014)
10. C. Gautier, P. Fichet, D. Menut, J. L. Lacour, D. L'Hermite, and J. Dubessy, Main parameters influencing the double-pulse laser-induced breakdown spectroscopy in the collinear beam geometry, *Spectrochim. Acta B* 60(6), 792 (2005)
11. D. K. Killinger, S. D. Allen, R. D. Waterbury, C. Stefano, and E. L. Dottery, Enhancement of Nd: YAG LIBS emission of a remote target using a simultaneous CO_2 laser pulse, *Opt. Express* 15(20), 12905 (2007)
12. Y. Yu, W. Zhou, and X. Su, Detection of Cu in solution with double pulse laser-induced breakdown spectroscopy, *Opt. Commun.* 333, 62 (2014)
13. R. Sattmann, V. Sturm, and R. Noll, Laser-induced breakdown spectroscopy of steel samples using multiple Q-switch Nd:YAG laser pulses, *J. Phys. D* 28(10), 2181 (1995)
14. X. Su, W. Zhou, and H. Qian, Optical emission character of collinear dual pulse laser plasma with cylindrical cavity confinement, *J. Anal. At. Spectrom.* 29(12), 2356 (2014)
15. A. Bogaerts, Z. Chen, and D. Autrique, Double pulse laser ablation and laser induced breakdown spectroscopy: A modeling investigation, *Spectrochim. Acta B* 63(7), 746 (2008)
16. A. De Giacomo, M. Dell'Aglio, D. Bruno, R. Gaudiuso, and O. De Pascale, Experimental and theoretical comparison of single-pulse and double-pulse laser induced breakdown spectroscopy on metallic samples, *Spectrochim. Acta B* 63(7), 805 (2008)
17. F. Colao, V. Lazic, R. Fantoni, and S. Pershin, A comparison of single and double pulse laser-induced breakdown spectroscopy of aluminum samples, *Spectrochim. Acta B* 57(7), 1167 (2002)
18. V. N. Rai, A. K. Rai, F. Y. Yueh, and J. P. Singh, Optical emission from laser-induced breakdown plasma of solid and liquid samples in the presence of a magnetic field, *Appl. Opt.* 42(12), 2085 (2003)
19. P. A. Benedetti, G. Cristoforetti , S. Legnaioli, V. Palleschi, L. Pardini, A. Salvetti, and E. Tognoni, Effect of laser pulse

energies in laser induced breakdown spectroscopy in double-pulse configuration, *Spectrochim. Acta B* 60(11), 1392 (2005)

20. B. Rashid, R. Ahmed, R. Ali, and M. A. Baig, A comparative study of single and double pulse of laser induced breakdown spectroscopy of silver, *Phys. Plasmas* 18(7), 073301 (2011)
21. H. Griem, Principles of Plasma Spectroscopy, Cambridge: Cambridge University Press, 1997
22. X. Li, Z. Wang, X. Mao, and R. E. Russo, Spatially and temporally resolved spectral emission of laser-induced plasmas confined by cylindrical cavities, *J. Anal. At. Spectrom.* 29(11), 2127 (2014)
23. NIST, Atomic Spectra Database, http://physics.nist.gov
24. V. I. Babushok, F. C. Jr DeLucia, J. L. Gottfried, C. A. Munson, and A. W. Miziolek, Double pulse laser ablation and plasma: Laser induced breakdown spectroscopy signal enhancement, *Spectrochim. Acta B* 61(9), 999 (2006)
25. W. Zhou, X. Su, H. Qian, K. Li, X. Li, Y. Yu, and Z. Ren, Discharge character and optical emission in a laser ablation nanosecond discharge enhanced silicon plasma, *J. Anal. At. Spectrom.* 28(5), 702 (2013)